



Deuteron beam interaction with lithium jet in a neutron source test facility¹

A. Hassanein

Argonne National Laboratory, 9700 South Cass Avenue, Argonne, IL 60439, USA

Abstract

Testing and evaluating candidate fusion reactor materials in a high-flux, high-energy neutron environment are critical to the success and economic feasibility of a fusion device. The current understanding of materials behavior in fission-like environments and existing fusion facilities is insufficient to ensure the necessary performance of future fusion reactor components. An accelerator-based deuterium–lithium system to generate the required high neutron flux for material testing is considered to be the most promising approach in the near future. In this system, a high-energy (30–40 MeV) deuteron beam impinges on a high-speed (10–20 m/s) lithium jet to produce the high-energy (≥ 14 MeV) neutrons required to simulate a fusion environment via the Li (d, n) nuclear stripping reaction. Interaction of the high-energy deuteron beam and the subsequent response of the high-speed lithium jet are evaluated in detail. Deposition of the deuteron beam, jet-thermal hydraulic response, lithium-surface vaporization rate, and dynamic stability of the jet are modeled. It is found that lower beam kinetic energies produce higher surface temperature and consequently higher Li vaporization rates. Larger beam sizes significantly reduce both bulk and surface temperatures. Thermal expansion and dynamic velocities (normal to jet direction) due to beam energy deposition and momentum transfer are much lower than jet flow velocity and decrease substantially at lower beam current densities.

1. Introduction

In current fusion reactor concepts, most of the energy released by fusion reactions is transported by high-energy neutrons that travel through a variety of materials from the first wall to the blanket and shield structure. An understanding of neutron effects in candidate materials is critical to the successful and reliable, safe, and prolonged operation of fusion reactors. The main problem stems from the high neutron-flux and high-energy spectrum unique to the D–T most-promising near-term fusion reaction. The flux of high-energy neutrons is predicted to cause a complex synergistic formation of extensive displacement and nuclear transmutation, which will have the effect of changing and degrading material properties, generating radioactive waste, and affecting the overall economic value of fusion energy [1].

Certain technical concerns of the D–Li neutron-source test facility are associated with interaction of the deuteron with the high-speed Li jet and the subsequent response of the Li jet. Primarily, the liquid Li target must first perform two basic functions: generate the neutrons through the D–Li stripping reaction, and remove the energy deposited by the deuteron beam. The approach is relatively simple. The accelerator-generated deuteron beam is directed toward a high-speed flowing jet of liquid Li, as shown in Fig. 1. This system must also be capable of operating under the high vacuum ($< 10^{-5}$ Torr) required by the accelerator technology. The Li flow passes through the beam interaction zone (defined by the beam size and shape, see Fig. 1), where it stops and absorbs the incident beam power and thus heats a portion of the Li. The Li continues to flow to a drain channel in a quench tank where complete mixing occurs with the large volume of Li in the tank. Some of the concerns are the resulting high temperature in the lithium jet at the interaction zone where excessive surface vaporization can occur, lithium sputtering or ejection due to beam bombardment, jet dynamic

¹ Work supported by the US Department of Energy, Office of Fusion Energy.

response due to deposited beam momentum, and resulting jet-thermal expansion due to heat deposition.

In this paper, the hydraulic and dynamic responses of the Li jet due to deuteron beam interaction are modeled and analyzed. The analysis is done parametrically for several beam energies, beam currents, beam sizes and shapes, and jet velocities to assess concept feasibility and reliability, compare with previous designs, and explore future upgrades. The analysis can be performed for either a free-falling jet or for the back-plate-supported jet of the former Fusion Materials Irradiation Test (FMIT) facility [2].

2. Beam–jet interaction

Deposition, and response of the Li jet to the bombardment of the deuterons, are simulated with the HIJET computer code, which is an enhanced and upgraded subset version of the comprehensive A*THERMAL computer code [3]. The HIJET code initially calculates the deposition of incident high-energy deuterons in a flowing Li target. The code calculates, using several analytical models, the energy loss of the deuteron ion beam through both electronic and nuclear stopping powers of the Li target atoms along its path. The analytical models use stopping cross sections that incorporate experimental data for accurate modeling of the deposition profile.

The HIJET code then calculates the detailed thermal response of the jet subject to various conditions. The code incorporates both finite-element and finite-difference solu-

tion methods to the heat conduction and hydrodynamics equations with advanced numerical techniques for more accurate and efficient solution. Detailed models to calculate surface vaporization and erosion rates of the Li jet are also implemented in the HIJET code [4].

3. Li-jet response

The flowing Li jet must be capable of performing the following functions: removing the heat deposited by the energetic deuterons at reasonable flow velocities, accommodating heat deposited with little thermal expansion to maintain jet integrity, and absorbing deuteron beam momentum without much distortion to its condition prior to beam interaction.

3.1. Thermal response

The thermal response of the Li jet is calculated by solving a time-dependent heat conduction equation, which is given by

$$\rho C_p \frac{\partial T}{\partial t} = \nabla \cdot (K \nabla T) + \dot{q} \quad (1)$$

where T is temperature, ρ is density, C_p is specific heat, K is thermal conductivity, and $\dot{q}(y, z, t)$ is the volumetric energy deposition rate of the incident deuteron beam. All thermophysical properties are assumed to be functions of local temperature. The deuteron range and power deposition profile are both strongly dependent on the initial

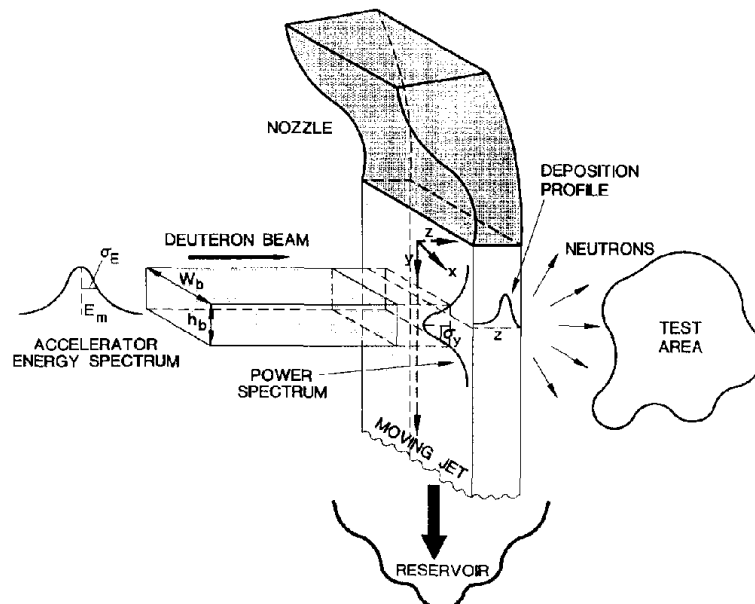


Fig. 1. Schematic illustration of beam on jet interaction assembly in a neutron-source test facility.

deuteron energy and energy distribution. The range of deuterons in the Li jet (z -direction) increases strongly with energy. Power density then increases substantially with decreasing deuteron initial energy. The Li jet thickness must then be tailored to the deuteron's initial energy to maximize neutron flux at the test facility, minimize Li flow rate, and ensure complete stopping of the incident beam. A finite spread in deuteron beam incident energy around a mean value (Gaussian distribution), while increasing the effective range, can significantly reduce peak energy deposition (Bragg's peak) near the end-of-range compared to that of a monoenergetic distribution [5]. The volumetric energy deposition function $\dot{q}(y, z, t)$ can be calculated for different incident energy spectra (z -direction) and for different power-shape spectra (y -direction) that may be required to mitigate the effects, if any, of the sudden high power deposition (square-pulse) on the cold Li target exiting the nozzle.

The jet's front-surface temperature (along the y -direction) will then be determined by the incident beam energy spectrum, beam current density, and beam power-shape along the flowing path. The evaporating Li flux leaving the jet surface is calculated in detail from models developed for nonequilibrium conditions [4]. The amount of Li mass evaporated must be minimized to maintain vacuum integrity, reduce beam–vapor interaction, and minimize Li vapor deposition on accelerator and other components of the system. The total amount of Li evaporated is not only restricted to beam exposure area (i.e., beam footprint $h_b \times W_b$), but also depends on the exposed area of the jet downstream after leaving the beam area and before entering the quench tank. In fact, a significant part of the Li vaporization mass will be derived from exposed areas after leaving the beam interaction zone. This is because the jet-surface temperature continues to rise after leaving the beam deposition region due to bulk heat conduction where most of the beam energy is deposited. Therefore, the exposed jet surface zone, immediately after the beam interaction zone, and just before entering the quench tank, should be kept to a minimum.

Fig. 2 shows the effect of the initial deuteron beam energy on the maximum temperature rise of the Li jet under the conditions shown. The deuteron energy range in Li decreases substantially as incident energy decreases. Varying the initial deuteron energy may be desirable to produce neutron spectra with different characteristics for a wide range of nuclear applications [6] and to optimize and accelerate the damage rate in the test area [7]. Lower incident deuteron energies deposit their energy near the surface, causing a higher surface temperature and consequently a higher Li vaporization mass. The vaporization rate is calculated for an area with a width equal to W_b and a height equal to the y -position and assuming a 100% duty factor. Fig. 3 shows the Li mass vaporized as a function of the exposed vertical distance along the jet surface, for a 5-cm beam height. The vaporization rate for deuteron

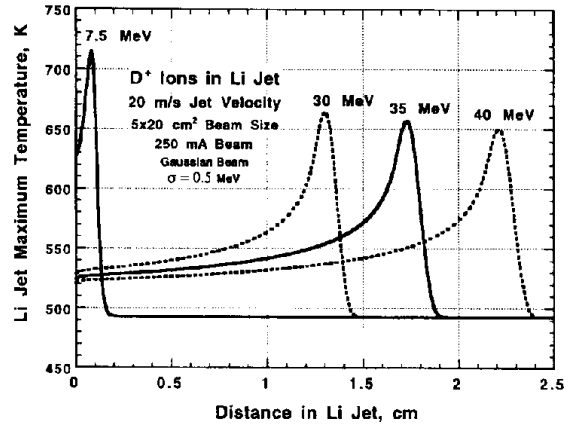


Fig. 2. Spatial distribution of Li maximum temperature for different beam incident energies.

incident energy of 30–40 MeV is < 1 g/yr for exposed vertical distances of up to 50 cm and a beam width of 20 cm.

Fig. 4 shows the evaporated Li mass as a function of the vertical distance along the jet surface (y -direction) for different beam sizes and jet velocities. Higher jet velocities reduce the temperature rise and therefore reduce vaporization flux. For the same beam current density a beam size with lower beam height (h_b) is recommended because the maximum surface and bulk temperatures will be much lower than those at a higher h_b . This is also important in reducing dynamic and thermal jet response to beam deposition. However, this must be taken into account in designing and arranging the test samples behind the Li jet. Fig. 5 shows the effect of the higher current density of the former FMIT design (smaller beam size, i.e., 1×3 beam at 100 mA) [2]. Because of the resulting high surface temperature due to higher current density (Fig. 6), the evaporated flux is much higher than that of lower current densities. The

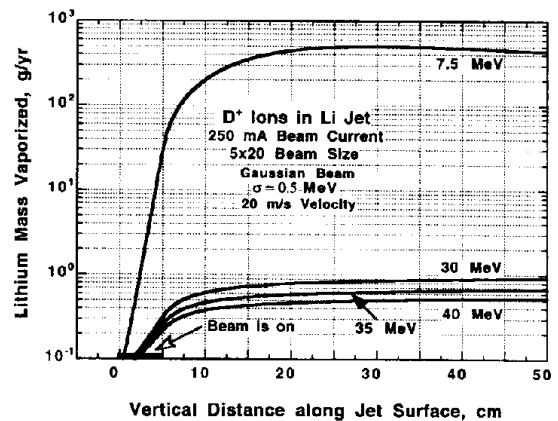


Fig. 3. Lithium vaporization rate along jet surface at different beam energies.

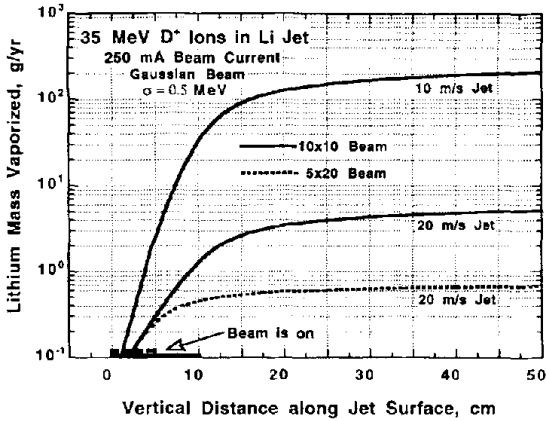


Fig. 4. Lithium vaporization rate at different beam sizes and jet velocities.

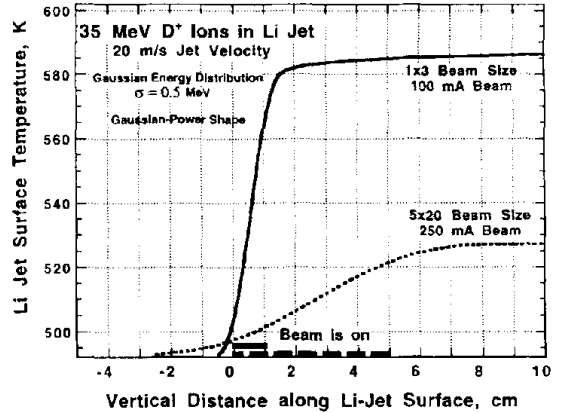


Fig. 6. Lithium surface temperature along jet surface for different beam sizes and beam currents.

implications of these vaporization rates (although seemingly insignificant) require further analysis to assess the impact on the vacuum system, accelerator performance, and vapor deposition and activation areas.

3.2. Jet thermal expansion

The heat deposited from the deuteron beam will cause the jet to expand thermally and generate internal-velocity profiles. The magnitude of the thermal expansion and the resulting velocity distributions are calculated by solving the mass conservation equation:

$$\frac{\partial \rho}{\partial t} + \nabla \cdot (\rho V) = 0 \tag{2}$$

where ρ is density and V is the resulting three-dimensional velocity profile generated inside the flowing jet. The resulting perturbation velocity in the y -direction will be superimposed on the main jet velocity and will slightly

help to increase the jet-flow speed. Of particular concern, however, is the resulting velocity perturbation in the z -direction, i.e., V_z . Higher V_z can cause jet distortion, increase jet instabilities, and degrade neutron performance in the test area.

To estimate the resulting maximum perturbation velocity in the z -direction, velocity in the x -direction is assumed negligible and that in the y -direction is assumed equal to jet-flow velocity. Eq. (2) can then be reduced to

$$\frac{\partial \rho}{\partial t} + V_y \frac{\partial \rho}{\partial y} + \frac{\partial (\rho V_z)}{\partial z} = 0. \tag{3}$$

All variables of Eq. (3) are treated as both time- and space-dependent. The equation is numerically solved with implicit methods, coupled with the heat conduction equation, for various incident beam and jet parameters.

Fig. 7 shows jet maximum expansion velocity (V_z) toward the front surface for different beam configurations. To obtain the maximum velocity, a back-plate-supported

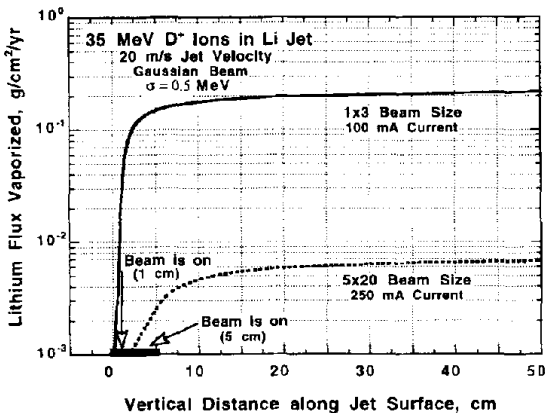


Fig. 5. Effect of beam size and beam current on Li vaporization rate.

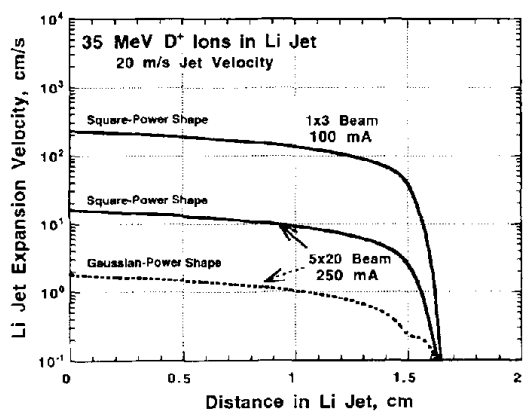


Fig. 7. Jet expansion velocity toward surface for different beam configuration and power profiles.

jet is assumed. The expansion velocity of the high-current-density beam (FMIT design) is about one order of magnitude higher than for the beam with lower current density. Higher expansion velocities normal to the flow direction may cause flow instabilities and jet disintegration, especially close to the nozzle exit. One solution for mitigating this effect is to use a Gaussian power profile along the flow direction instead of a flat profile, as shown in Fig. 1. Fig. 7 also shows that a Gaussian power shape further reduces the jet expansion velocity at the location of first beam-on-target interaction. The maximum jet expansion thickness is, however, much less than 1 mm in the z -direction for the larger beam size at the end of the beam interaction zone.

3.3. Jet mechanical response

The deuteron-beam-deposited momentum in the Li jet will also force the jet to move and generate internal velocity perturbation. The magnitudes of these velocities are calculated by solving the momentum conservation equation:

$$\rho \frac{\partial V}{\partial t} + \rho V \cdot \nabla V + \nabla P = F \quad (4)$$

where P is pressure and F is the generated body force per unit volume. F is mainly in the z -direction and is given by the rate of change of momentum. The deuteron beam momentum at depth z , M_z , is given by

$$M_z = m_d V_d = \sqrt{2 m_d E_z} \quad (5)$$

where m_d is deuteron mass, V_d is deuteron velocity, and E_z is deuteron energy at depth z . By ignoring the pressure generated by the body force and considering only the

resulting velocity in the z -direction, Eq. (4) can be reduced to

$$\frac{\partial V_z}{\partial t} + V_y \frac{\partial V_z}{\partial y} + V_z \frac{\partial V_z}{\partial z} = \frac{\phi_d m_d}{\rho} \frac{dV_d}{dz} \quad (6)$$

where ϕ_d is the incident deuteron flux. Fig. 8 shows resulting jet velocities normal to jet flow and due to beam-deposited momentum. The calculated velocities shown in the z -direction are for a free jet, i.e., no back-plate support. Lower current densities also result in lower velocities normal to jet flow. The magnitude of momentum-induced velocities is usually lower than the thermal expansion velocities produced from heat deposition. Nevertheless, velocity perturbations due to both jet thermal expansion and momentum deposition are small for the larger-size and lower-current-density beam and should not affect beam stability.

4. Conclusions

Interaction of the high-energy deuteron beam with the lithium jet for the accelerator-based neutron source has been modeled and analyzed. Deuteron energy deposition and thermal response of the Li target have been calculated parametrically for various beam and target configurations. Larger beam sizes reduce jet thermal load and increase the allowable test volume. Surface vaporization generally seems to be low and decreases with higher beam energies, lower beam-current densities, and higher jet velocities. Calculated velocity perturbations due to jet thermal expansion and beam-deposited momentum are small and may not affect beam stability. Other issues that require further study include jet instabilities due to nozzle erosion and design, and effect of Li vaporization and condensation on accelerator performance and on the vacuum system.

References

- [1] P. Schiller, Fusion Eng. Design 30 (1995) 191.
- [2] J.A. Hassberger, Preliminary Assessment of Interactions Between the FMIT Deuteron Beam and Liquid Lithium Target, HEDL-TME 82-28 (Hanford Engineering Development Laboratory, Richland, WA, March 1983).
- [3] A. Hassanein, J. Nucl. Mater., 122–123 (1984) 1453.
- [4] A. Hassanein et al., Nuclear Eng. Design/Fusion 106 (1984) 307.
- [5] A. Hassanein and D. Smith, J. Nucl. Mater., 212–215 (1994) 1671.
- [6] K. Noda et al., J. Nucl. Mater., 179–181 (1991) 1147.
- [7] I.C. Gomes and D.L. Smith, Studies of D–Li Neutron Source—An Overview, Argonne National Laboratory Report ANL/FPP/TM-267 (June 1994).

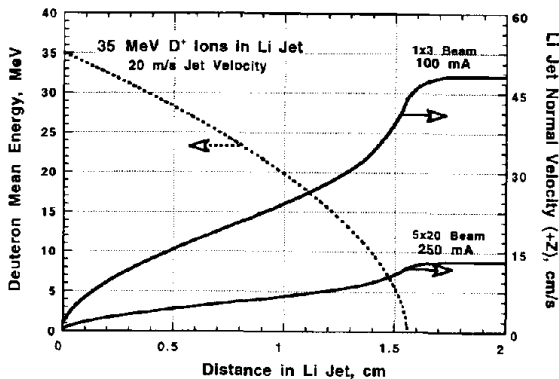


Fig. 8. Jet normal velocity due to beam-deposited momentum for different beam configurations.